

Technical Progress Report: Completion of Spectral Rotating Shadowband Radiometers and Analysis of Atmospheric Radiation Measurement Spectral Shortwave Data

*J. Michalsky and L. Harrison
Atmospheric Sciences Research Center
University at Albany, State University of New York
Albany, New York*

Abstract

Our goal in the Atmospheric Radiation Measurement (ARM) Program is the improvement of radiation models used in general circulation models (GCMs), especially in the shortwave, 1) by providing improved shortwave radiometric measurements for the testing of models and 2) by developing methods for retrieving climatologically sensitive parameters that serve as input to shortwave and longwave models.

At the Atmospheric Sciences Research Center (ASRC) in Albany, New York, we are acquiring downwelling direct and diffuse spectral irradiance, at six wavelengths, plus downwelling broadband longwave, and upwelling and downwelling broadband shortwave irradiances that we combine with National Weather Service surface and upper air data from the Albany airport as a test data set for ARM modelers. We have also developed algorithms to improve shortwave measurements made at the Southern Great Plains (SGP) ARM site by standard thermopile instruments and by the multifilter rotating shadowband radiometer (MFRSR) based on these Albany data sets.

However, the major objective of our program has been the development of two spectral versions of the rotating shadowband radiometer. The MFRSR contains six filtered detectors, and one unfiltered silicon detector that serves as a surrogate total shortwave sensor. The MFRSR was completed in the first phase of this program and is deployed at the SGP cloud and radiation testbed (CART) site. It has been selected as the core instrument of the ARM solar and infrared observing system (SIROS) radiation instrument suite that is being deployed at each of twenty extended facilities within the SGP CART site. The rotating shadowband spectroradiometer (RSS) contains a 256-channel diode array that spans the wavelengths 350-1050 nm with resolution varying between 0.6 nm and

8 nm. The prototype of the RSS has acquired data on the roof of the ASRC at the State University of New York in Albany, but a field-worthy unit is not yet complete. A calibration facility for these instruments is being built at the ASRC to characterize cosine response, to determine absolute spectral calibration, and to characterize spectral response. The facility is operational, and upgrades are continuing.

The MFRSR, which was developed during the first years of the ARM Program, has become a workhorse at the CART sites in Oklahoma and Kansas, and it is widely deployed in other climate programs. We have spent most of our effort this year developing techniques to retrieve column aerosol, water vapor, and ozone from direct beam spectral measurements of the MFRSR. Additionally, we have had success in calculating shortwave surface albedo and aerosol optical depth from the ratio of direct to diffuse spectral irradiance. Using the surface albedo and the global irradiance, we have calculated cloud optical depths. From cloud optical depth and liquid water measured with the microwave radiometer, we have calculated effective liquid cloud particle radii. In each case, we have attempted to validate our approach using independent measurements or retrievals of the parameters under investigation. With the exception of the ozone inter-comparison, the corroborative measurements have been made at the SGP CART site. This report highlights these results.

ASRC Data Acquisition

A small part of our ARM funding is used to acquire a high-quality radiation data set on the roof of the ASRC using the MFRSR and the same standard thermopile pyranometers and pyrhemometers that are used at the SGP CART site. With the instruments accessible we are able to provide frequent cleaning, alignment, and calibration to

ensure a high-quality data set. The data have been used to test longwave and shortwave radiation models in a GCM. They allow testing of hardware and firmware changes to the MFRSR before they are implemented at the SGP CART site. They have enabled us to develop algorithms to improve both the accuracy of shortwave irradiance measurements made by the MFRSR and thermopile instruments.

The calibration of all of our shortwave sensors is tied to our absolute cavity radiometer. Last September we took part in the ARM absolute cavity intercomparison at the National Renewable Energy Laboratory. Although a final report has not been published, the preliminary results suggest that our absolute cavity agrees with the world standard to about 0.2%. This result validates the measurements used in the studies described here.

The shortwave and longwave downwelling radiation models in the Global Environmental and Ecological Simulation of Interactive Systems GCM have been tested for many clear days with the result that downwelling shortwave radiation is overestimated by about 20–30 W/m², and the downwelling longwave model largely agrees with measurements. The shortwave results from the ASRC GCM modeling team led by W. C. Wang are similar to those of Betts et al. (1993). Other unpublished results suggest similar conclusion.

The first-class thermopile radiation data at ASRC were used to derive a methodology to improve shortwave measurements made using the MFRSR unfiltered silicon detector. Temperature control of the detector and cosine response corrections as implemented in the MFRSR produced root-mean-square errors of about 11, 10, and 16 W/m² in the total, diffuse, and direct irradiances before spectral correction. Spectral correction further improved 1993 total and diffuse irradiance rms errors by about 20%. Mt. Pinatubo aerosols, however, no longer affected shortwave radiation in 1995, and the spectral corrections now appear to lower the errors in total and diffuse irradiance by about 50%.

Until recently, diffuse irradiance measurements made at the SGP CART site were a problem because tracking disks did not block the direct beam reliably. Improved trackers should solve the problem; however, the archived downwelling shortwave irradiances, which are best measured by summing diffuse and direct horizontal irradiances, are suspect. We have tested a procedure that uses direct and total horizontal measurements and a one-time measurement of the angular response of the total horizontal pyranometer to make improved shortwave measurements. Comparisons with our carefully monitored tracking disk

diffuse measurements confirm the validity of this approach.

Instrument Development

The RSS prototype that we have developed uses a prism spectrometer and a charge-coupled device (CCD) photodiode array to measure 256 continuous wavelength intervals from 350 to 1050 nm. This instrument is intended for deployment at the central sites. A prototype of this instrument has been machined, assembled, and briefly tested in the laboratory and outdoors. The test results are very encouraging with the spectral resolution and instrument sensitivity very close to design values. With the departure of our post-doctoral student who had responsibility for this instrument, we have fallen behind schedule. Nevertheless, we expect to have the RSS operational on the ASRC roof before the end of the year.

Calibration

Radiometric calibration and characterization of our spectral instruments requires the development of three test platforms to measure the angular response, the spectral sensitivity, and the absolute response. All are computer controlled by the software Labview®. All of these facilities are operational; however, we expect to spend more effort improving the spectral response measurements. Currently, the output of the monochromator is below our expectations. The angular response and absolute calibration facilities are operating satisfactorily.

Analysis

Aerosol Optical Depth

Five of the six filters in an MFRSR may be used for the measurement of aerosol optical depth. When the atmosphere is clear and stable, Langley analysis is possible. The Bouguer-Lambert-Beer law is given by

$$I = I_0 e^{-\tau \cdot m} \quad (1)$$

where I is the spectral irradiance as measured by the MFRSR, I_0 is the spectral irradiance that the MFRSR would measure at the top of the atmosphere, τ is the total optical depth from all sources of extinction, and m is the air mass relative to the zenith direction. If the atmosphere is stable, a plot of the natural log of I versus m yields a linear plot whose slope is the total optical depth τ and whose intercept is I_0 . I_0 may be obtained from a standard lamp or derived from Langley plots according to the above procedure on occasions when the atmosphere is stable.

When the atmosphere is free of clouds, but unstable because of changing aerosol conditions, we may calculate τ using this measured I_o . We have used our estimate of I_o to calculate the averages of thirty-minute time series of optical depth. We allow the optical depth to change linearly in time, but if any point deviates by more than ± 0.01 optical depths from this linear behavior, we advance one time step and test the series again. When we find thirty minutes of data that satisfy the criterion, we advance thirty minutes and begin the search again. Figure 1 is a plot of daily averages of these thirty-minute samples.

Water Vapor

Reagan et al. (1987) introduced the modified Langley technique as an independent method of calculating total column water vapor using the 940-nm water band in the near infrared. Bruegge et al. (1992) followed the Reagan method, but used LOWTRAN7 to calculate transmission in their water vapor passband. We have followed the procedure of Bruegge et al. (1992), but used MODTRAN2 for our transmission calculations. Derived water vapor column abundances for 104 clear mornings or afternoons have been

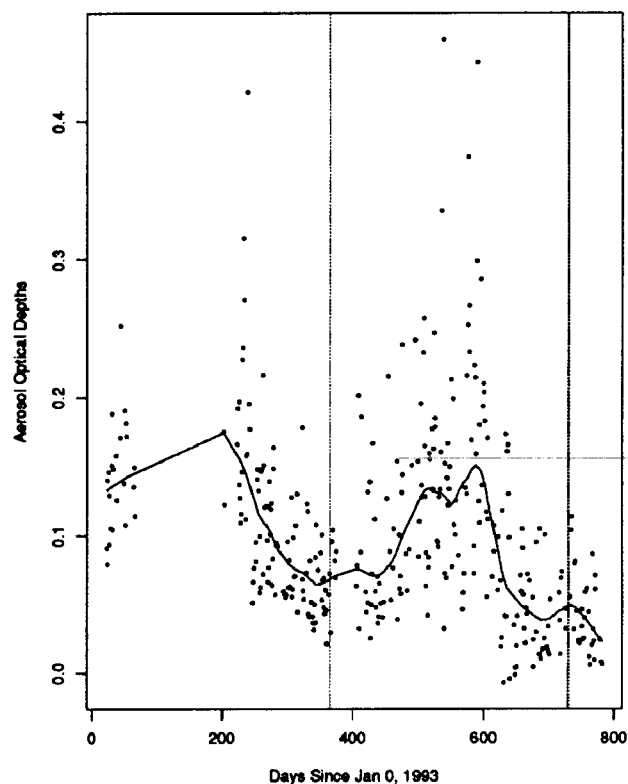


Figure 1. Daily-averaged aerosol optical depths at 500 nm for SGP central facility.

compared to water vapor columns derived from microwave measurements made simultaneously at the SGP CART site central facility. These measurements span a year and cover the range of water vapor experienced at the SGP site. Figure 2 is a plot of the MFRSR-derived water vapor versus the microwave radiometer measurements for the same times.

Ozone

Ozone may also be derived using the five filters used in the aerosol optical depth derivation above. Realistic aerosol size distributions produce little curvature on a plot of the natural log of the aerosol optical depth versus the natural log of the wavelength at which the optical depth is measured. This can be shown theoretically, and it is our experience experimentally. King and Byrne (1976) suggested that one could estimate this wavelength dependence with a quadratic function in these variables. By perturbing the ozone optical depth until a best quadratic fit is obtained, we can derive an estimate of ozone column abundance. Figure 3 is a plot of ozone column for the last four months of 1994 for the Dobson spectrophotometer at Mauna Loa Observatory and for the MFRSR. The Dobson is a standard for ozone measurements.

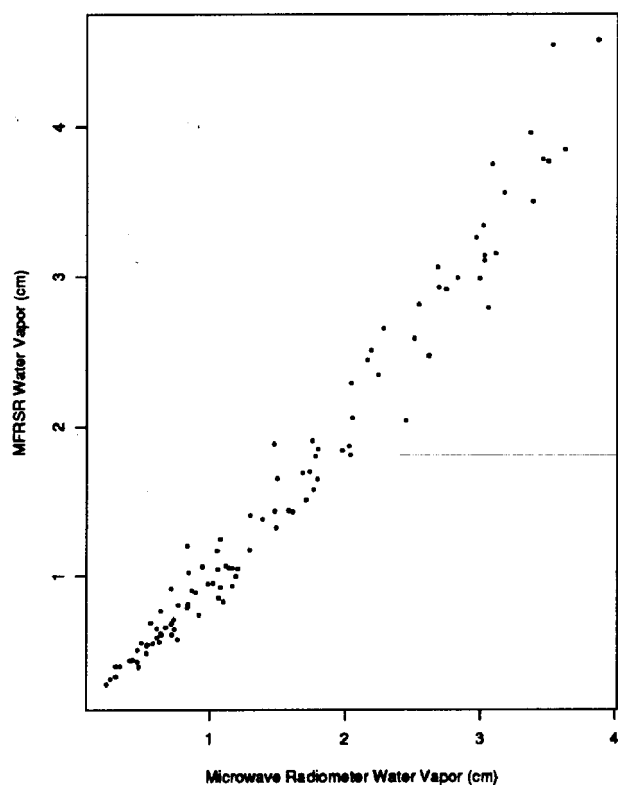


Figure 2. MFRSR-derived water vapor versus microwave radiometer water vapor at SGP.

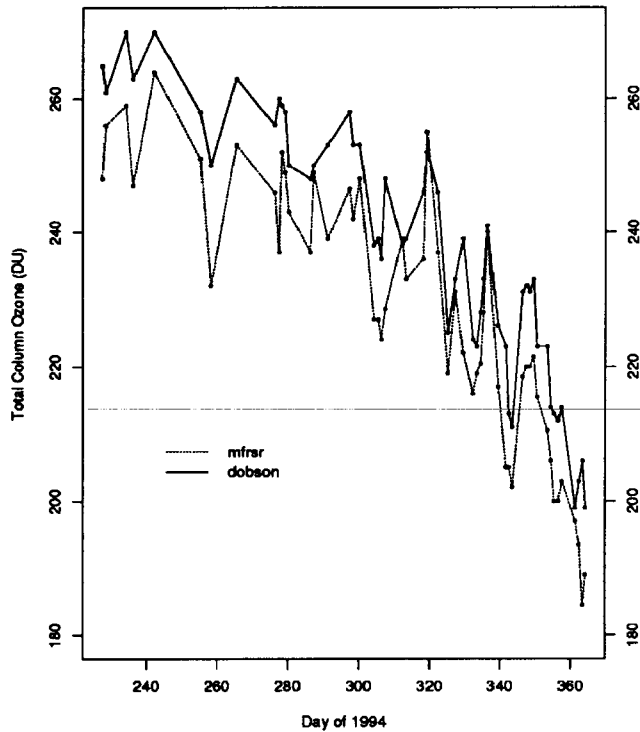


Figure 3. Mauna Loa Observatory total column ozone from the Dobson spectrometer and the MFRSR.

Radiative Transfer and Surface Albedo

A certain amount of received solar radiation is multiply scattered, requiring a more rigorous treatment of scattering processes through the use of radiative transfer models that include all orders of multiple scattering. However, full radiative transfer computations are extremely time-consuming, limiting the applications of the radiative transfer model. Noting that the response of interest is merely the downward surface flux which is characterized by very large data bases (i.e., as a function of solar zenith angle), we developed the adjoint formulation of discrete ordinate radiative transfer to understand the measurements of the MFRSR.

Based on the definition of adjoint operator, $\langle I^*, LI \rangle = \langle L^* I^*, I \rangle$, we constructed a variational principle for the forward radiative transfer equation. It led to the adjoint formulation of the radiative transfer equation, $L^* I^* = \Sigma$, with appropriate boundary conditions. The adjoint operator is

$$L^*(Z, \Omega) = -\mu \frac{d}{dz} + \beta^{\text{ext}} - \beta^{\text{sca}} \int_{4\pi} d\Omega' p(z, -\Omega' \rightarrow -\Omega) \quad (2)$$

and the adjoint source for the downward diffuse irradiance is

$$\Sigma = -\mu \sigma(z) U(-\mu). \quad (3)$$

The downward diffuse irradiance, $G[I]$, can be evaluated as equation

$$G[I] = \langle \Sigma, I \rangle = \langle L^* I^*, I \rangle = \langle I^*, LI \rangle = \langle I^*, Q \rangle \quad (4)$$

To calculate the radiative effects of m different sources, we must solve the forward radiative transfer equation m times. However, such effects can be evaluated by solving the adjoint radiative transfer equation once and undertaking m inner products instead. It is demonstrated that the accuracy of the adjoint method is equal to that of the forward discrete ordinate radiative transfer method, and the computing time is significantly reduced.

The irradiance at the surface, as well as the diffuse/direct ratio, nonlinearly depends upon several factors such as wavelength, solar zenith angle, surface albedo, and atmospheric species including ozone, cloud, and aerosol. We employed the adjoint method of radiative transfer in conjunction with the nonlinear least squares method to infer the surface albedo and the aerosol optical depth simultaneously from the ratio of diffuse to direct irradiances. We processed the data at wavelengths of 415, 500, 610, and 665 nm for the time intervals during which there is a clear stable atmosphere devoid of any cloud cover for a long enough period of time for the air mass to undergo a large change, particularly on the days in which the optical depths are large. We compared the inferred surface albedo with measurements at the SGP site of ARM and the inferred optical depth with the results of Langley regression. The data in Table 1 show reasonable agreement, when cloud-free conditions prevail.

Cloud Properties

Once the parameters related to surface albedo and aerosol have been retrieved, we can use the same approach to infer stratified cloud properties under cloud-covered sky. Specifying the single scattering albedo and the asymmetry factor based on Mie theory, we can infer the cloud optical depth from the global irradiance. We selected the transmittance of the atmosphere, the ratio of measured global irradiance to the solar constant, as the inversion function to avoid the uncertainties of absolute calibration.

Table 1. Summary of the observed and inferred surface albedo and total optical depth during August 1994 at SGP.						
Time	Wavelength	Surface Albedo			Optical Depth	
		$\lambda(\text{nm})$	NLSM	A_{10m}	A_{25m}	NLSM
940816	415	0.036±0.013	0.031	0.038	0.487±0.009	0.503±0.009
	500	0.066±0.011	0.048	0.063	0.285±0.006	0.299±0.004
	610	0.128±0.016	0.071	0.109	0.198±0.007	0.214±0.004
	665	0.162±0.019	0.079	0.126	0.144±0.007	0.162±0.004
940821	415	0.094±0.007	0.025	0.032	0.584±0.004	0.589±0.012
	500	0.088±0.007	0.045	0.052	0.372±0.004	0.373±0.004
	610	0.122±0.010	0.069	0.089	0.263±0.004	0.266±0.004
	665	0.137±0.009	0.074	0.105	0.197±0.004	0.207±0.004

We compared our inferred cloud optical depth with Geostationary Operational Environmental Satellite (GOES) measurements at the SGP site during April 1994. Temporal variations of our results, shown in Figure 4, are consistent with that of GOES measurements. However, our results are slightly higher, which may be due to the effects of spatial average of GOES measurements over a 0.3° by 0.3° area.

Publications and Presentations

The following publications and presentations were completed between November 1, 1994 and October 31, 1995: Harrison, L., J. Michalsky, and J. Berndt. 1994. Automated multifilter rotating shadow-band radiometer: An instrument for optical depth and radiation measurements, *Appl. Opt.*, **33**, 5118-5125.

Harrison, L., and J. Michalsky. 1994. Objective algorithms for the retrieval of optical depths from ground-based measurements, *Appl. Opt.*, **33**, 5126-5132.

Michalsky, J. J., L. C. Harrison, and W. E. Berkheiser III. 1995. Cosine response characteristics of radiometric and photometric sensors, *Solar Energy*, **54**.

Michalsky, J. J., J. C. Liljegren, and L. C. Harrison. 1995. A comparison of sun photometer derivations of total column water vapor and ozone to standard measures of same at the Southern Great Plains Atmospheric Radiation Measurement Site, *Journal of Geophysical Review-Atmospheres*, in revision.

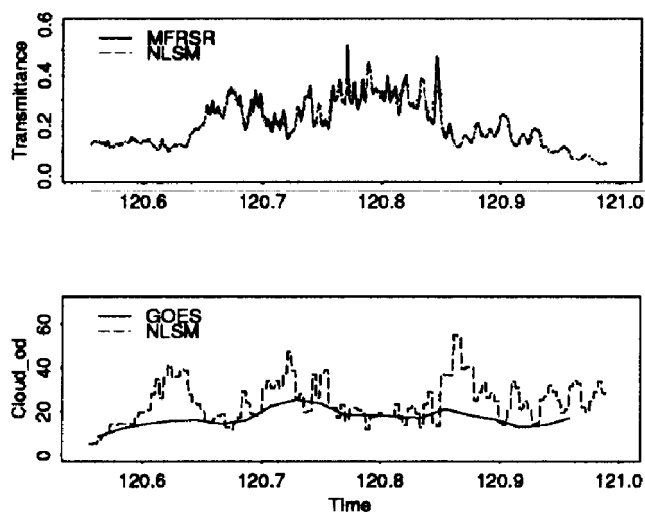


Figure 4. Measured and fitted transmittances and inferred cloud optical depths on April 30, 1994, at SGP.

Zhou, Chuan, and Joseph Michalsky. 1995. Spectral correction of silicon photodiode solar radiation detectors, *Solar Energy*, in revision.

Four papers have been presented since the last annual report:

Michalsky, J. J., J. A. Schlemmer, N. R. Larson, L. C. Harrison, W. E. Berkheiser III, and N. S. Laulainen. 1994. Measurement of the seasonal and annual variability of total column aerosol in a northeastern network. In *Proceedings of the International Specialty Conference Aerosols and Atmospheric Optics: Radiative Balance and Visual Air Quality, 26-30 September 1994, Snowbird, Utah*. W. Malm (ed). Air and Waste Management Association, Pittsburgh, Pennsylvania, pp. 247-258.

Michalsky, J., and H. Harrison. 1995. Total column ozone retrieval from the visible chappuis band: Comparisons with standard ultraviolet measurements. In *Optical Remote Sensing of the Atmosphere, Vol. 2, 1995*, OSA Technical Digest Series, Optical Society of America, Washington, D.C., pp. 195-197.

Michalsky, J. J., and E. Dutton. 1995. Comparison of standard and MFRSR sunphotometry at Mauna Loa Observatory. In *Climate Monitoring and Diagnostics Laboratory Annual Meeting*, March 8-9, 1995.

Michalsky, J., L. Harrison, Q. Min, J. Schlemmer, W. Berkheiser III, and C. Zhou. 1995. Rotating shadow-band radiometer development and analysis of spectral shortwave data. In *Atmospheric Radiation Measurement Science Team 5th Annual Meeting*, March 20-23, 1996.

Acknowledgment

This work was performed under U.S. Department of Energy Grant No. DE-FG02-90ER61072.

References

Betts, A. K., J. H. Ball, and A. C. M. Beljaars. 1993. Comparison between the land surface response of the ECMWF Model and the FIFE-1987 data, *Quar. J. Roy. Met. Soc.*, **119**, 975-1001.

Bruegge, C. J., J. E. Conel, R. O. Green, J. S. Margolis, R. G. Holm, and G. Toon. 1992. Water vapor column abundance retrievals during FIFE, *J. Geophys. Res.*, **97**, 18759-18768.

King, M. D., and D. M. Byrne. 1976. A method for inferring total column ozone from the spectral variation of total optical depth obtained with a solar radiometer, *J. Atmos. Sci.*, **33**, 2242-2251.

Reagan, J. A., K. Thome, B. Herman, and R. Gall. 1987. Water vapor measurements in the 0.94 micron band: Calibration, measurements and data applications. In *Proceedings of the International Geosciences Remote Sensing Symposium*, IEEE 87CH 2434-9, 63-67.